Full Paper

www.molinf.com

molecular informatics

DOI: 10.1002/minf.201500043

Identification of Lead Compounds as Inhibitors of STAT3: Design, Synthesis and Bioactivity

Antonio Botta,[a] Esther Sirignano,[a] Ada Popolo,[a] Carmela Saturnino,*[a] Stefania Terracciano,[a] Antonio Foglia,[a] Maria Stefania Sinicropi,[b] Pasquale Longo,[c] and Simone Di Micco*[a]

Abstract: STAT3 belongs to the signal transducers and activators of transcription (STAT) family. It has been demonstrated that STAT3 is constitutively activated in many tumors, playing a role in carcinogenesis and tumor progression. For this reason, it has being considered a potential target for cancer therapy. In this context, we have designed, synthesized and evaluated 1,4-dimethyl-carbazole derivatives, targeting the STAT3 protein. Moreover, MTT assay performed on A375 and HeLa, showed significant antiproliferative activity of some of synthesized compounds (**3**–**5**). The same compounds (**3**–**5**) considerably reduced STAT3 expression, as demonstrated by Western blot analysis. Our multidisciplinary approach shows that 1,4-dimethyl-carbazoles are potential building blocks to develop more affinity ligands of STAT3.

Keywords: STAT3 · STAT3 inhibitor · Molecular docking · Antitumor compound · 1,4-dimethyl-carbazoles

1 Introduction

The protein family of signal transducers and activators of transcription (STAT), whose members include STAT1–STAT4, STAT5A, STAT5B and STAT6, are activated by extracellular signals such as cytokines, growth factors and hormonal factors. These factors bind to cell-surface receptors leading to autophosphorylation of a tyrosine residue. STAT proteins contain a SH2 domain, which recognizes the receptor phosphotyrosine, and in this way are recruited from the cytosol and associate with the activated receptor. This recruitment is followed by STAT3 phosphorylation on a carboxy-terminal tyrosine, either directly by the receptor or by a receptor-associated JAK kinase. Tyrosine phosphorylation of STATs induces their dimerization and translocation to the nucleus, where they bind to specific promoter sequences in target genes inducing their expression.[1–3] In particular, the SH2 domain of STAT3 is responsible of the dimerization, by recognition of Pro-pTyr-Leu-Lys-Thr-Lys sequence of the other monomer.[4,5] Recently, it has been demonstrated that the constitutively unphosphorylated STAT3 (uSTAT3) is active in gene control,[6] and its involvement in oncogenesis and biological function in tumor cells has already reported.[7–9] These new data highlight uSTAT3 as a new practicable target for small molecules in cancer therapy.

In human tumors, a high frequency of STAT1, STAT3, and STAT5 activation is seen. Classified as oncogene, STAT3 is widely recognized as a master regulator of molecular and biological events leading to the generation of cancer phenotypes.[10] The constitutive activation of STAT3 is frequently detected in primary human breast carcinoma cells, and elevated levels of STAT3 phosphorylation have been correlated with tumor invasion, nodal metastasis, and staging ($P < 0.05$).[11,12] Moreover, the inhibition of STAT3 induces the death of tumor cells.[10,12] Thus, these evidences suggest STAT3 as an attractive molecular target for the development of novel cancer therapeutics. The disruption of oncogenic STAT3 signaling may theoretically be accomplished through various approaches, involving direct and indirect strategies. Many attempts have been done to develop STAT3 inhibitors,[13] including: peptidomimetics[14–17] and non-peptide inhibitors[18–22] of STAT3-SH2 domain, inhibitors of the DNA-binding domain of STAT3.[23,24] It is also been reported a strategy to indirectly block STAT3 by using modulators of the upstream components of the STAT3 pathway.[1,25–28] Despite many efforts to develop STAT3 inhibitors,

[a] *A. Botta, E. Sirignano, A. Popolo, C. Saturnino, S. Terracciano, A. Foglia, S. Di Micco*
Dipartimento di Farmacia, Università degli Studi di Salerno
Via Giovanni Paolo II 132, 84084 Fisciano, Salerno, Italy
phone/fax: +39 089969176 (S. D. M.); +39 089969769 (C. S.); +39 089969602 (fax)
**e-mail: saturnino@unisa.it*
sdimicco@unisa.it

[b] *M. S. Sinicropi*
Dipartimento di Chimica e Biologia, Università degli Studi di Salerno Via Giovanni Paolo II 132, 84084 Fisciano, Salerno, Italy

[c] *P. Longo*
Dipartimento di Farmacia e Scienze della Salute e della Nutrizione, Università della Calabria
87036 Arcavacata di Rende, Cosenza, Italy

Supporting information for this article is available on the WWW under http://dx.doi.org/10.1002/elan.201500043.

there are no small molecules targeting this protein approved by the FDA so far.

In this context, we have tried to identify new chemical fragments to develop more druggable STAT3 modulators. Our strategy has focused on the design of non-peptidic small building blocks, which present a better ADME properties respect to peptides and peptidomimetics.

It is noteworthy that carbazole derivatives show different biological profiles, such as: inhibition of proinflammatory cytokine biosynthesis; antiproliferative effect on SVR (murine endothelial cells) cells;[31] cytotoxic activity against human solid cancer cells (PC3, DU145, and PA-1),[32] murine leukemia L1210 cell line,[33] human leukemic topoisomerase II sensitive (HL60N) and resistant (HL60 MX2) cell lines,[34] SK-N-SH human neuroblastoma (NB) cells.[35] Due to these multi-biological activities, the carbazole scaffold is considered a privileged structure,[29] thus, able to bind different classes of macromolecules with high affinity depending on the appropriate pattern of chemical substitutions. These premises make the carbazole scaffold very attractive for lead discovery of new agents against different tumor cells.

Recently, some of us have proposed some complex carbazoles as lead compounds for STAT3 inhibition.[29,30] Our aim is to get more druggable STAT3 inhibitors with respect to the previously proposed lead compounds[29] (**11** and **12**, Figure S1) presenting a quite high molecular weight (~500 u.a.). For this reason, any further modifications, by introducing new substituents, should improve the affinity for the macromolecule to the detriment of bioavailability. Moreover, in the previous work[29] the chemical features of the substituents for an efficient decoration of the carbazole scaffold have not been delineated. On this premise, being the carbazole an easily obtainable privileged chemical core with a potential biological activity, we designed new simplified 1,4-dimethyl-carbazoles showed in Figure 1 (**1**–**10**). In particular, our starting point (see below) was the 1,4-dimethyl-carbazole (**1**) from which we tried to get more structural information about the minimum structural elements responsible for the binding to the macromolecular target to develop new STAT3 inhibitors with improved bioactivities and bioavailability.

2 Material and Methods

2.1 Computational Studies

All ligands (**1**–**10**) were sketched using the graphical interface Maestro version 6.0, Schrödinger, LLC, New York, NY, 2003, and their geometries optimized through MacroModel 8.5[36] by using the MMFFs force field[37] and the Polak–Ribier conjugate gradient algorithm (maximum derivative less than 0.001 kcal/mol). A GB/SA (generalized Born/surface area) solvent treatment[38] was used, mimicking the presence of H_2O in the geometry optimization.

The crystal structure of STAT3β homodimer bound to DNA (PDB ID: 1BG1)[39] was used as macromolecule in the theoretical studies. By graphical interface Maestro the protein was prepared for the docking calculations: the DNA and water molecules were deleted, all hydrogens were added, bond order and missing atoms were checked through visual inspection, and the charges of side chains were attributed according to their p*K*a.

Molecular docking studies were performed using AutoDock 4.2 software.[40] To get a representative conformational space during the docking calculations and taking into account the variable number of active torsions, 10 calculations consisting of 256 runs were performed, obtaining 2560 structures for each ligand (**1**–**10**). The Lamarckian genetic algorithm was employed for dockings, along with an initial population of 700 randomly placed individuals. The maximum number of energy evaluations and of generations was set up at 6×10^6 and 7×10^6, respectively. A mutation rate of 0.02, a crossover rate of 0.8, and the local search frequency of 0.26 were used. Results differing by less than 2 Å in positional root-mean-square deviation (*rmsd*) were clustered together and ranked by free energy of binding. For all the docked structures, all bonds were treated as active torsional bonds. The grid box was sized at $64\times64\times64$ number of points, by using 0.375 Å between the grid points. The *x*, *y*, and *z* coordinates of grid center were: 96.616, 73.201 and 68.027.

2.2 Chemistry

All reagents and solvents were purchased from Sigma-Aldrich s.r.l. (Milan, Italy). The elemental analyses for C, H and N were recorded on a ThermoFinnigan Flash EA 1112 series and performed according to standard microanalytical procedures. ^{1}H NMR, ^{1}HCOSY and ^{13}C NMR spectra were recorded at 298 K on a Bruker Avance 300 Spectrometer operating at 300 MHz (^{1}H) and 75 MHz (^{13}C) and referred to internal tetramethylsilane.

2.2.1 General Procedures for the Synthesis of Compounds 1–5[41]

5-substituted-1H-indole (6.60 mmol) was dissolved in ethanol (20 mL) and stirred at room temperature. To this solution hexan-2,5-dione (8.18 mmol) and 4-methylbenzenesulfonic acid (8.24 mmol) were added. The mixture was stirred under reflux for 4 h. After the reaction, the solution was cooled, and the solvent was evaporated, poured into water and extracted with diethyl ether (3 x 30 mL). The organic layer was dried over anhydrous $MgSO_4$, filtered and the solvent removed by evaporation. The resulting residue was purified on a silica gel column chromatography in hexane/ethyl acetate (7 : 3).

All NMR data are in according to literature ones.

*Synthesis of 5,8-dimethyl-9H-carbazole-3-sulfonyl chloride (**18**)*

1,4-dimethyl-9H-carbazole (**1**) (2.56 mmol) was dissolved in chloroform (20 mL). The solution was cooled to 0 °C. To

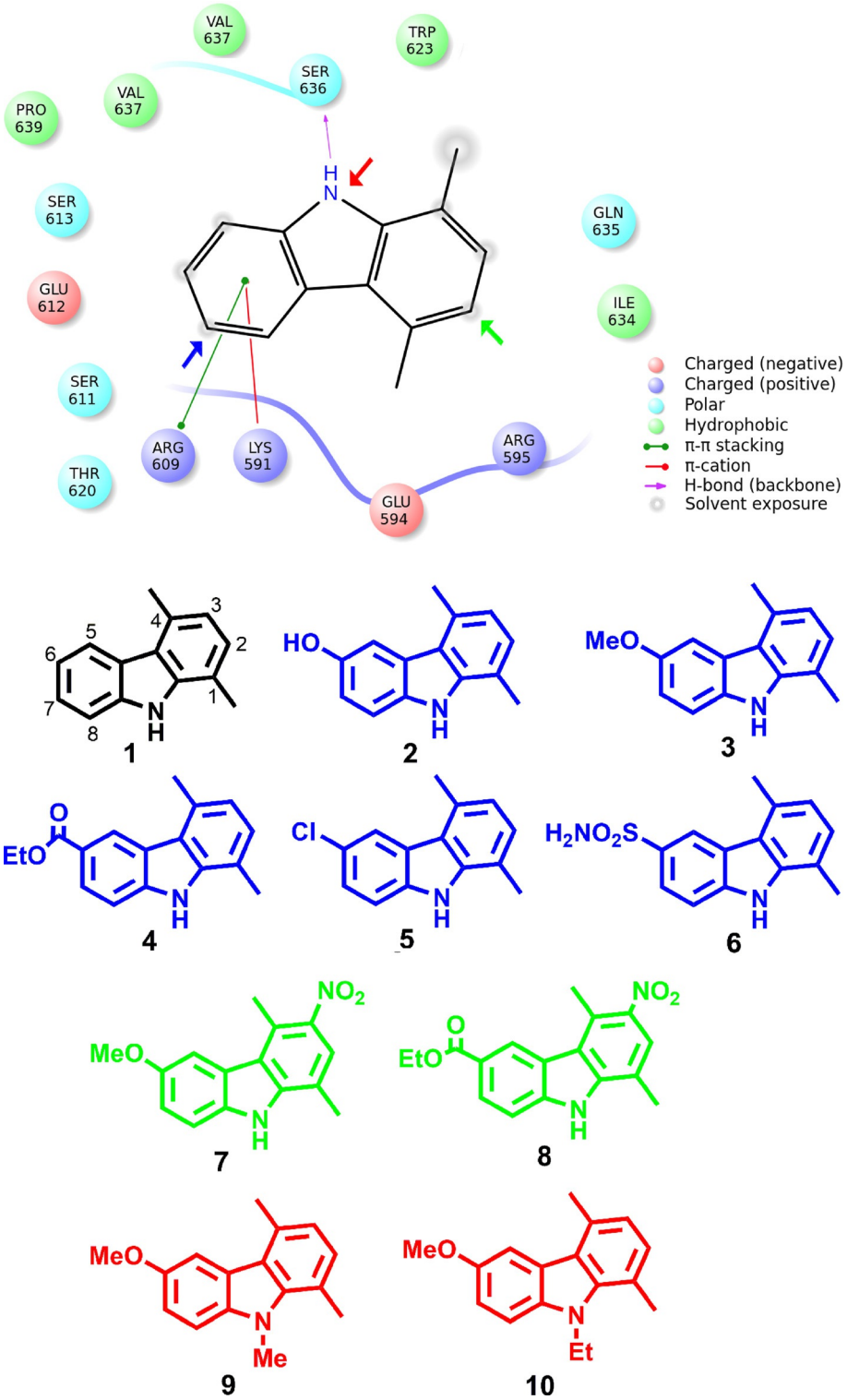

Figure 1. 2D panel representing interactions between **1** and STAT3, and molecular structures of compounds **1**–**10**. The blue, green and red arrows indicate the chemical modification positions on compound **1** to obtain the derivatives (**1**–**10**, accordingly colored), respectively: **2**–**6**; **7** and **8**; **9** and **10**.

this solution chlorosulfonic acid (9.76) was added and the mixture was stirred at room temperature for 30 min. After the reaction the solution was cooled, poured into water and extracted with chloroform (3×30 mL). The organic layer was dried over anhydrous $MgSO_4$, filtered and the solvent removed by evaporation to give a white solid.

^{1}H NMR (δ_{ppm} $CDCl_3$ 250 MHz): 2.57 [(ClOOS-C_6H_3-C_6H_2-(CH_3)$_2$-NH 3H,s]; 2.89 [(ClOOS-C_6H_3-C_6H_2-(CH_3)$_2$-NH 3H,s]; 6.96–7.42 [(ClOOS-C_6H_3-C_6H_2-(CH_3)$_2$-NH 5H,m]; 8.01 [(ClOOS-C_6H_3-C_6H_2-(CH_3)$_2$-*NH* 1H,s].

^{13}C NMR (δ_{ppm} THF-d_8 689 MHz): 16.55 [(ClOOS-C_6H_3-C_6H_2-(CH_3)$_2$-NH]; 20.46 [(ClOOS-C_6H_3-C_6H_2-(CH_3)$_2$-NH]; 110.37–137.28 [(ClOOS-C_6H_3-C_6H_2-(CH_3)$_2$-NH].

Elemental analysis: calcd. for $C_{14}H_{12}ClNO_2S$ (%): C, 57.24; H, 4.12; N, 4.77. Found (%): C, 57.81; H, 4.15; N, 4.81.

*Synthesis of 5,8-dimethyl-9H-carbazole-3-sulfonamide (**6**)*

5,8-dimethyl-9H-carbazole-3-sulfonyl chloride (**18**) (4.68 mmol) was dissolved in 15 mL of tetrahydrofuran. To this solution 0.08 mL of a 2 M ammonia solution in ethanol was added. The mixture was stirred at room temperature for 2 h. After the reaction the solution was evaporated and purified on a silica gel column chromatography in hexane/ethyl acetate (8 : 2).

^{1}H NMR (δ_{ppm} THF-d_8 250 MHz): 2.51 [(NH_2OOS-C_6H_3-C_6H_2-(CH_3)$_2$-NH 3H,s]; 2.79 [(NH_2OOS-C_6H_3-C_6H_2-(CH_3)$_2$-NH 3H,s]; 6.80–7.44 [(NH_2OOS-C_6H_3-C_6H_2-(CH_3)$_2$-NH 5H,m]; 8.12 [(NH_2OOS-C_6H_3-C_6H_2-(CH_3)$_2$-NH 1H,s]; 10.18 [(NH_2OOS-C_6H_3-C_6H_2-(CH_3)$_2$-*NH* 1H,s].

^{13}C NMR (δ_{ppm} THF-d_8 689 MHz): 16.55 [(NH_2OOS-C_6H_3-C_6H_2-(CH_3)$_2$-NH]; 20.46 [(NH_2OOS-C_6H_3-C_6H_2-(CH_3)$_2$-NH]; 110.37–139.58 [(NH_2OOS-C_6H_3-C_6H_2-(CH_3)$_2$-NH].

IR (KBr) (cm^{-1}): 3482 [(*NH_2OOS*-C_6H_3-C_6H_2-(CH_3)$_2$-NH];

Elemental analysis: calcd. for $C_{14}H_{14}N_2O_2S$ (%): C, 61.29; H, 5.14; N, 10.21. Found (%): C, 61.90; H, 5.19; N, 10.29.

*Syntehsis of 6-methoxy-1,4-dimethyl-3-nitro-9H-carbazole (**7**)*

1,4-dimethyl-9H-carbazole (**1**) (2.22 mmol) was dissolved in 20 mL of acetic anhydride and then cooled to 0–5 °C. To this solution fuming HNO_3 100% (2.22 mmol) was added dropwise to give a dark solution. The reaction mixture was stirred at room temperature overnight. Then the mixture was filtered and dried in vacuum and then washed with diethyl ether (3×10 mL) to give an orange solid.

^{1}H NMR (δ_{ppm} $CDCl_3$ 250 MHz): 2.57 [(CH_3O-C_6H_3-C_6H_2-(CH_3)$_2$-NO_2-NH, 3H, s]; 3.05 [(CH_3O-C_6H_3-C_6H_2-(CH_3)$_2$-NO_2-NH, 3H, s]; 4.01 [(*CH_3*O-C_6H_3-C_6H_2-(CH_3)$_2$-NO_2-NH, 3H, s]; 7.89–8.18 [(CH_3O-*C_6H_3*-*C_6H_2*-(CH_3)$_2$-NO_2-NH, 4H, m]; 9.97 2.57 [(CH_3O-C_6H_3-C_6H_2-(CH_3)$_2$-NO_2-*NH*, 1H, s].

^{13}C NMR(δ_{ppm} $CDCl_3$ 689 MHz): 14.5 [(CH_3O-C_6H_3-C_6H_2-(CH_3)$_2$-NO_2-NH]; 15.3 [(CH_3O-C_6H_3-C_6H_2-(CH_3)$_2$-NO_2-NH]; 55.8 [(*CH_3*O-C_6H_3-C_6H_2-(CH_3)$_2$-NO_2-NH]; 103.0–162.3 [(CH_3O-*C_6H_3*-*C_6H_2*-(CH_3)$_2$-NO_2-NH].

Elemental analysis: calcd. for $C_{15}H_{14}N_2O_3$ (%): C, 66.66; H, 5.22; N, 10.36. Found (%): C, 67.32; H, 5.27; N, 10.46.

*Synthesis of ethyl-5,8-dimethyl-9H-carbazole-3-nitro-carboxylate (**8**)*

The synthesis of **8** was carried out with the same procedure used for **7** by reacting ethyl-5,8-dimethyl-9H-carbazole-3-carboxylate with fuming HNO_3 in stoichiometric amount.

^{1}H NMR (δ_{ppm} $CDCl_3$ 250 MHz): 2.57 [(CH3-CH_2-OOC-C_6H_3-C_6H_2-(*CH_3*)$_2$-NO_2-NH, 3H, s]; 3.05 [(CH_3O-C_6H_3-C_6H_2-(*CH_3*)$_2$-NO_2-NH, 3H, s]; 4.01 [(*CH_3*O-C_6H_3-C_6H_2-(CH_3)$_2$-NO_2-NH, 3H, s]; 7.89–8.18 [(CH_3O-*C_6H_3*-*C_6H_2*-(CH_3)$_2$-NO_2-NH, 4H, m]; 9.97 2.57 [(CH_3O-C_6H_3-C_6H_2-(CH_3)$_2$-NO_2-*NH*, 1H, s].

^{13}C NMR(δ_{ppm} $CDCl_3$ 689 MHz): 14.5 [(CH_3-CH_2-OOC-C_6H_3-C_6H_2-(*CH_3*)$_2$-NO_2-NH]; 15.3 [(CH_3-CH_2-OOC-C_6H_3-C_6H_2-(*CH_3*)$_2$-NO_2-NH]; 18.2 [(*CH_3*-CH_2-OOC-C_6H_3-C_6H_2-(CH_3)$_2$-NO_2-NH]; 60.9 [(CH_3-*CH_2*-OOC-C_6H_3-C_6H_2-(CH_3)$_2$-NO_2-NH]; 103.0–169.5 [(CH_3-CH_2-OOC-C_6H_3-C_6H_2-(*CH_3*)$_2$-NO_2-NH].

Elemental analysis: calcd. for $C_{18}H_{19}N_2O_4$ (%): C, 66.04; H, 5.85; N, 8.56. Found (%): C, 66.56; H, 5.90; N, 8.64.

*Synthesis of 6-methoxy-1,4,9-trimethyl-carbazole (**9**)*

1,4-dimethyl-9H-carbazole (**1**) (1.82 mmol) was dissolved in anhydrous dimethylformamide and stirred at room temperature for 10 min. To the solution at 0 °C sodium hydride (60% dispersion in mineral oil) (2.72 mmol) was added. The solution was warmed up to room temperature and 0.37 mL of iodomethane (5.47 mmol) were added and stirred at room temperature for 1 h. Then the mixture was poured into water and extracted with ethyl acetate (3×30 mL). The organic layer was dried over anhydrous $MgSO_4$, filtered and the solvent removed by evaporation to give a white solid.

^{1}H NMR (δ_{ppm} $CDCl_3$ 250 MHz): 2.51 [(CH_3O-C_6H_3-C_6H_2-(*CH_3*)$_2$-N-CH_3 3H,s]; 2.79 [(CH_3O-C_6H_3-C_6H_2-(*CH_3*)$_2$-N-CH_3 3H,s]; 3.83 [(*CH_3*O-C_6H_3-C_6H_2-(CH_3)$_2$-N-CH_3 3H,s]; 4.1 [(CH_3O-C_6H_3-C_6H_2-(CH_3)$_2$-N-*CH_3* 3H,s]; 6.86–7.34 [(CH_3O-C_6H_3-C_6H_2-(CH_3)$_2$-N-CH_3 5H,m].

^{13}C NMR (δ_{ppm} $CDCl_3$ 689 MHz): 16.55 [(CH_3O-C_6H_3-C_6H_2-(*CH_3*)$_2$-N-CH_3]; 20.47 [(CH_3O-C_6H_3-C_6H_2-(*CH_3*)$_2$-N-CH_3]; 55.34 [(*CH_3*O-C_6H_3-C_6H_2-(CH_3)$_2$-N-CH_3]; 44.3 [(CH_3O-C_6H_3-C_6H_2-(CH_3)$_2$-N-*CH_3*]; 105.44–153.65 [(CH_3O-C_6H_3-C_6H_2-(CH_3)$_2$-N-CH_3].

Elemental analysis: calcd. for $C_{16}H_{17}NO$ (%): C, 80.30; H, 7.16; N, 5.85. Found (%): C, 81.02; H, 7.23; N, 5.91.

*Synthesis of 6-methoxy-1,4-dimethyl-9-ethyl-carbazole (**10**)*

The synthesis of **10** was carried out with the same procedure used for **9**.

^{1}H NMR (δ_{ppm} $CDCl_3$ 250 MHz): 2.51 [(CH_3O-C_6H_3-C_6H_2-(*CH_3*)$_2$-N-CH_2-CH_3 3H,s]; 2.79 [(CH_3O-C_6H_3-C_6H_2-(*CH_3*)$_2$- N-CH_2-CH_3 3H,s]; 3.83 [(*CH_3*O-C_6H_3-C_6H_2-(CH_3)$_2$- N-CH_2-CH_3 3H,s]; 4.4 [(CH_3O-C_6H_3-C_6H_2-(CH_3)$_2$- N-*CH_2*-CH_3 3H,s]; 2.3 [(CH_3O-C_6H_3-C_6H_2-(CH_3)$_2$- N-CH_2-*CH_3* 3H,s] 6.86–7.34 [(CH_3O-C_6H_3-C_6H_2-(CH_3)$_2$- N-CH_2-CH_3 5H,m].

^{13}C NMR (δ_{ppm} $CDCl_3$ 689 MHz): 14.7 [(CH_3O-C_6H_3-C_6H_2-(*CH_3*)$_2$-N-CH_2-CH_3]; 20.47 [(CH_3O-C_6H_3-C_6H_2-(CH_3)$_2$-N-CH_2-*CH_3*];16.55 [(CH_3O-C_6H_3-C_6H_2-(*CH_3*)$_2$-N-CH_2-CH_3]; 20.47 [(CH_3O-C_6H_3-C_6H_2-(*CH_3*)$_2$-N-CH_2-CH_3]; 55.34 [(CH_3O-C_6H_3-C_6H_2-(*CH_3*)$_2$-N-CH_2-CH_3]; 44.3 [(CH_3O-C_6H_3-C_6H_2-(CH_3)$_2$-N-*CH_2*-CH_3]; 105.44–153.65 [(CH_3O-C_6H_3-C_6H_2-(*CH_3*)$_2$-N-CH_2-CH_3].

Elemental analysis: calcd. for $C_{17}H_{19}NO$ (%): C, 80.60; H, 7.56; N, 5.53. Found (%): C, 80.68; H, 7.63; N, 5.58.

2.3 Pharmacology

2.3.1 Antiproliferative Activity

Human melanoma (A375) and human epithelial cervix adenocarcinoma (HeLa) cell lines (3.5×104 cells/well) were plated on 96-well microtiter plates and allowed to adhere at 37 °C in a 5 % CO_2 atmosphere for 2 h.

Thereafter, the medium was replaced with 50 mL of fresh medium and a 75 mL aliquot of serial dilution of each test compound was added and then the cells incubated for 72 h. In some experiments, serial dilutions of cis-platin were added. Mitochondrial respiration, an indicator of cell viability, was assessed by the mitochondrial-dependent reduction of [3-(4,5-dimethylthiazol-2-yl)-2,5-phenyl-2H-tetrazolium bromide] (MTT) to formazan and cells viability was assessed accordingly to the method previously described (JPP).

Briefly 25 mL of MTT (5 mg/mL) were added and the cells were incubated for additional 3 h. Thereafter, cells were lysed and the dark blue crystals solubilised with 100 mL of a solution containing 50% (v:v) *N*,*N*-dimethylformamide, 20% (w:v) SDS with an adjusted pH of 4.5. The optical density (OD) of each well was measured with a microplate spectrophotometer (Titertek Multiskan MCC/340) equipped with a 620 nm filter. The viability of each cell line in response to treatment with tested compounds and Doxorubicin, used as positive control drug, was calculated as: % dead cells = 100−(OD treated/OD control)×100.

2.3.2 Western Blot Analysis

A375 and HeLa cells (7×10^5) were plated and allowed to adhere for 4 hours in DMEM 10% FBS. Designed compounds (50 μM) were monitored for 24, 48 or 72 hours. Total intracellular proteins were extracted from the cells by freeze/thawing in lysis buffer (Tris–HCl 50 mM pH 7.4) containing 10 mM NaF, 150 mM NaCl, 1% Nonidet P40, 1 mM phenylmethylsulfonylfluoride, 1 mM sodium orthovanadate, leupeptin (10 μg/mL) and trypsin inhibitor (10 μg/mL). Protein content was estimated according to Bio-Rad protein assay (BIO-RAD, Milan Italy) and 50 μg protein/lane were loaded onto an acrylamide gel and separated by SDS-PAGE in denaturing conditions. Blots were incubated with primary antibody anti-STAT3 (1:200), anti-pSTAT3 (1:200), anti-JAK2 (1:500), and anti Bcl2 (1:200). Primary antibody anti-GAPDH (1:3000) was used as loading control (Santa Cruz Biotechnology, DBA Italy). After incubation period with the primary antibodies and washing in TBS/0.1% Tween, the appropriate secondary antibody, (anti-rabbit for STAT3, mouse for pSTAT3, JAK2 and Bcl2, either 1:5000) was added for 1h at room temperature. Immunoreactive protein bands were detected by chemiluminescence using enhanced chemilumunescence reagents (ECL) in LAS 4000 (GE Healthcare).

3 Results and Discussion

3.1 Computer-Aided Design of 2–10

Our aim is to discover new ligands of SH2 domain of STAT3, as this domain is responsible of the protein dimerization, where a monomer recognizes the Pro-Tyr/pTyr-Leu-Lys-Thr-Lys sequence of its partner. In the recognition process a key role is played by Tyr705/phosphor Tyr705 (pY705). Thus, for our virtual screening, we have considered the protein region accommodating the Pro-Tyr/pTyr-Leu-Lys-Thr-Lys sequence and specially the interactions involving the Tyr705/pTyr705. In particular, the superimposition of uSTAT3 and pSTAT3 revealed that the two resolved structures are completely aligned (0.43 Å, Figure S2 Supporting Information).[6] Compared to pTyr705, it was observed a 2.0 Å shift of the unphosphorylated tyrosine side chain away from the phosphate binding pocket forming less contacts with its partner (Figure S3 Supporting Information).[6] Moreover it reported a lower binding affinity for uSTAT3:uSTAT3 formation compared to pSTAT3 dimer.[6] To design the compounds **2**–**10** (Figure 1), we used the compound **1** as our starting scaffold. By means of molecular docking, we obtained a three dimensional **1**-STAT3 model, in order to get structural suggestions to decorate the scaffold **1**. From the docked pose of **1**, we observed that the position 6 of carbazole ring (Figure 1) faces the cavity accommodating the Tyr705/pTyr705 (pY705, Figure 1). In details, the Tyr705/pY705 is accommodated in a small cavity, making crucial interactions with the side chains of Lys591, Arg609, Ser611, Glu612 and Ser613 (Figure S3,4 Supporting Information). Thus, we designed compounds **2**–**6** inserting at C-6 a hydrogen bond acceptor to mimic the key interactions observed for Tyr705/pTyr705, responsible for the protein-protein association. Taking into account the structural requirement and the synthetic feasibility, we introduced different substituents (**2**–**6**, Figure 1) to explore the influence on the interactions with the macromolecular counterparts. We inserted a hydroxyl, a methoxy, an ethyl ester groups, and a chlorine and a sulfonamide function (Figure 1). In addition to C-6 position, we observed that the position 3 of carbazole is close to the side chain of Arg595 (Figure 1). Thus, we decided to investigate the C-3 position to further improve the binding to the protein. For this purpose, we designed the compounds **7** and **8**, considering the easy introduction of a nitro group able to interact with Arg595 (Figure 1).

Beyond the fundamental interaction of the side chain of Tyr705/pTyr705, the Pro-Tyr/pTyr-Leu-Lys-Thr-Lys sequence donates a H-bond using NH of Leu706 to the backbone C=O of Ser636. The Leu706 also establishes van der Waals contacts with side chain of Trp623 and Val637. Thus, while in the design of compounds **2**–**8** we aimed to mimic the H-bond formed by Leu706 by NH of carbazole moiety, in **9** and **10** we tried to increase the contacts with STAT3 through van der Waals interactions by introducing alkyl

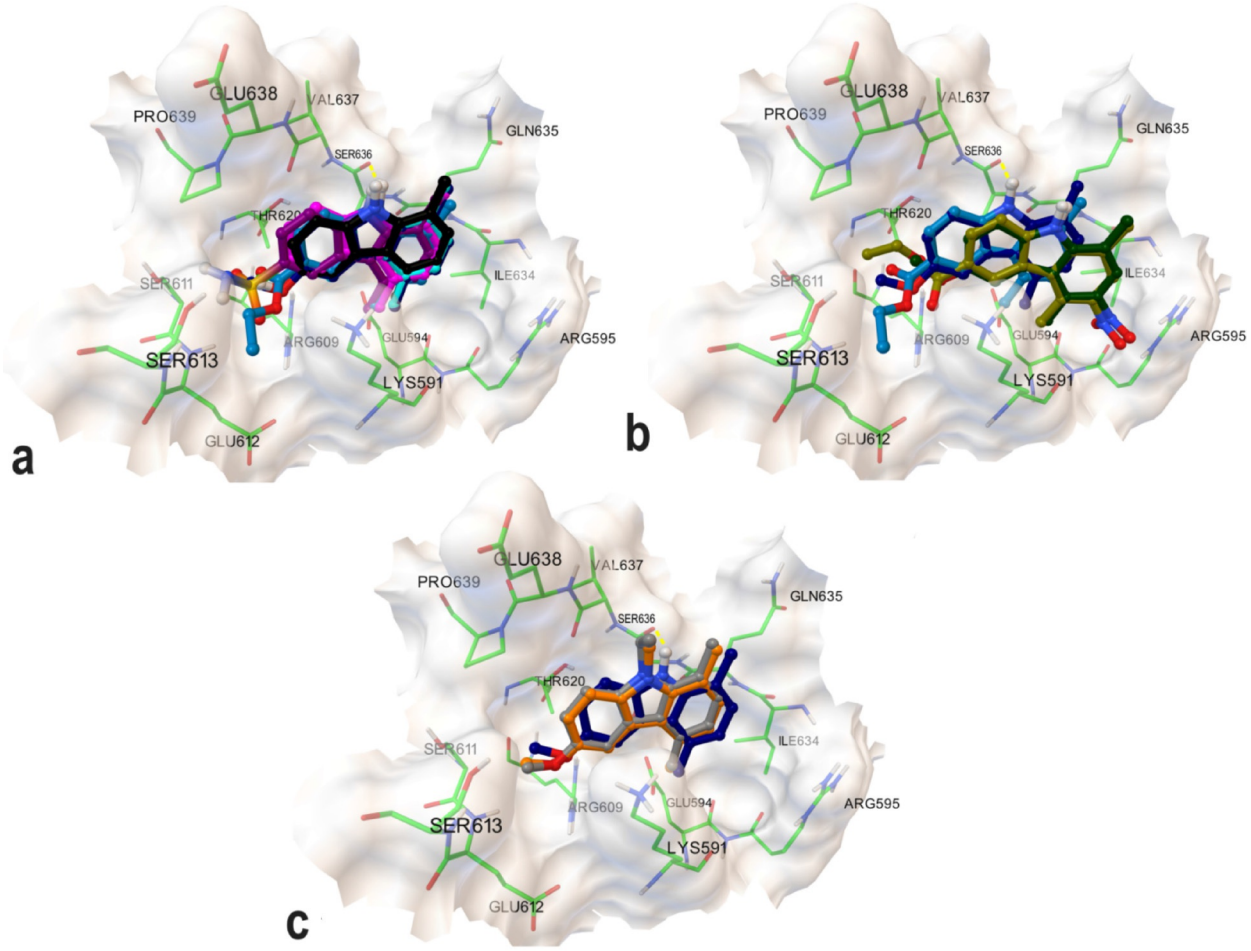

Figure 2. Superimposition in the STAT3 SH2 domain: a) **1**–**6**; b) **3**, **4**, **7** and **8**; c) **3**, **9** and **10**. The protein is represented by white molecular surface and tube (coloured: C, green; polar H, white; N, blue; O, red). All ligands are depicted by sticks (**1**, black; **2**, cyan; **3**, dark-blue; **4**, indigo; **5**, pink; **6**, purple; **7**, forest green; **8**, khaki; **9**, orange; **10**, grey) and balls (coloured by atom type: polar H, white; O, red; N, blue; S, yellow; Cl, light green). The C atoms of the **1**–**10** are coloured as for the sticks. The yellow dashed lines indicate the hydrogen bonds between ligands and protein. The figure highlights the common and different interactions made by **1**–**10** with STAT3 SH2 domain.

groups on the nitrogen (Figure 1) to the detriment of hydrogen bond. The designed compounds **2**–**10** were docked into the binding cavity of STAT3 (Figure 2, S5–S10 Supporting Information). The docked poses of **2**–**10** result well accommodated into protein binding cavity and seem to respect the predicted interactions from our design.

3.2 Chemistry

Compounds **1**–**5** were synthesized according to the Cronwell and Saxton reaction (see Scheme 1).[41] Compounds **18** was synthesized starting from compound **1** by reaction with chlorosulfonic acid at 0 °C (see Scheme 2). Compound **6** was obtained from **18** by reaction with a stoichiometric amount of a 2 M ammonia solution in ethanol (see Scheme 2). Compounds **7** and **8** were synthesized starting from compound **3** by reaction with sodium hydride at 0 °C in DMF and iodomethane to obtain compound **7** and with sodium hydride at 0 °C in DMF and iodoethane to obtain

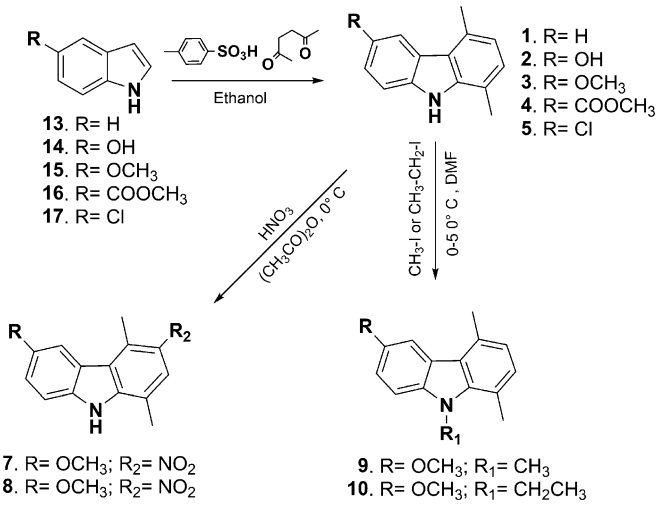

Scheme 1. Synthetic route for the preparation of compounds: **1**–**5**; **7**–**10**.

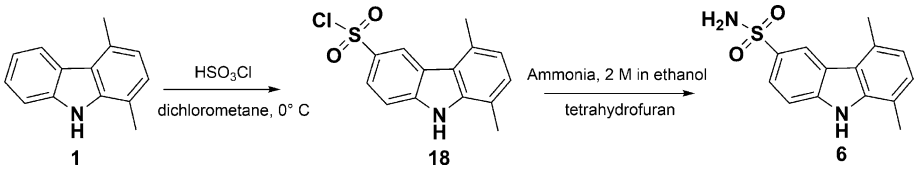

Scheme 2. Synthetic route for the preparation of compounds **6** and **18**.

compound **8** (See Scheme 1). Compound **9** and **10** were synthesized by reaction of compound **3** and **4** with a stoichiometric amount of fuming nitric acid in acetic anhydride[32] (see Scheme 1).

As revealed by NMR spectroscopy and elemental analysis, the synthesized compounds (see Experimental Section) were in accordance with the proposed molecular formulas.

3.3 Pharmacology

In order to analyze the biological activity of our new set of carbazole derivatives, antiproliferative assays have been carried out on all synthesized compounds (**1**–**10**). The growth inhibition activities of compounds **1**–**10** have been evaluated on human melanoma (A375) and human epithelial cervix adenocarcinoma (HeLa) cell lines, which constitutively express STAT3. The IC_{50} value, expressed as μM, is the concentration of compound that affords a 50% reduction in cell growth as compared to control cells (Table 1). Doxorubicin is also included as reference compound.

Compound **1** presents a comparable antiproliferative activity to doxorubicin on A375 and does not inhibit the growth of the remaining cell line. The small molecule **2** inhibits the cell growth of A375 similarly to the doxorubicin. On the HeLa cell line, the compound **2** shows a lower inhibition of cell growth with respect to doxorubicin. As shown in Table 1, compounds **3** and **5** show a comparable inhibitory activity on HeLa cells respect to doxorubicin, and better profile than reference on A375. In particular, **3** and **5** perform better than doxorubicin against A375 cell line. Compound **4** presents a similar antiproliferative activity to doxorubicin vs. A375. Compounds **6**, **7** and **9** have no antiproliferative activity: $IC_{50} > 100$ μM against two cell lines. Concerning **8**, we only observed a very low inhibition activity on A375 cells. Comparable cell growth inhibition activities to doxorubicin are shown by **10** on A375 cells, and presents a two-fold increase in IC_{50} with respect to doxorubicin on HeLa cells.

In order to verify the effect on STAT3 signaling pathways by our compounds, Western blot (see also Supporting Information) analysis was performed on cell lines A375 and HeLa. In particular, we selected the most interesting compounds (**3**–**5**) as emerged by MTT assay, along with the parent carbazole **1**. As negative control, we tested compound **7**, which has a nitro group in position 3. The compounds **3**–**5** showed a significant inhibition of STAT3 expression (Table 2) compared to the control cells, and the best inhibitory effect on the expression of STAT3 was observed after 72 hours. On the contrary, as expected, **1** and **7** do not look to interfere with STAT3, confirming the data obtained with MTT assay. Under the same experimental conditions, we evaluated the activity of these compounds on the expression of pSTAT3, JAK2 and Bcl2 but no significant results were obtained (Table 2). Compounds **3**–**5** significantly reduce STAT3 expression (>90%) in A375 cell line (Table 2). On HeLa cell line no significant inhibition was observed for compound **3**, while **4** and **5** showed an important inhibitory effect (45%) on STAT3 expression, even though at lesser extent respect to the data on A375 cells

Table 1. The IC_{50} values (μM) for **1**–**10** against A375 and HeLa cell lines are reported. The doxorubicin was used as reference compound. Results are expressed as mean ± *SEM* from at least three independent experiments, each performed in triplicate. Data were analyzed by Student's *t* test. [a] denotes $P < 0.005$ and [b] denotes $P < 0.001$ vs. doxorubicin on the same cell lines.

Compound	Cell line	
	A375	HeLa
1	80.0 ± 2.1	> 100
2	90.0 ± 3.0	80.0 ± 1.5
3	50.0 ± 2.6 [b]	70.0 ± 1.2
4	90.0 ± 3.9	60.0 ± 3.7
5	60.0 ± 1.9 [a]	60.0 ± 0.98
6	> 100	> 100
7	> 100	> 100
8	80.0 ± 4.6	90.0 ± 5.1
9	> 100	> 100
10	80.0 ± 1.9	> 100
Doxorubicin	87.0 ± 3.3	48.0 ± 3.1

Table 2. The percentage of STAT3 inhibition vs. control was calculated for the selected compounds. A375 and Hela cell lines were treated with the selected compounds, (**1**, **3**–**5**, **7**) and STAT3 expression was evaluated by Western blot analysis. Data for pSTAT3, JAK2 and Bcl2, not reported, as no significant activity was obtained (1–3%) even at higher concentrations (100 μM). Results are expressed as mean ± *SEM* of percentage of inhibition of STAT3 expression of three independent experiments.

Compound	A375	HeLa
1	2.0 ± 1.1	1.20 ± 0.75
3	94.33 ± 3.50	3.53 ± 1.80
4	90.66 ± 1.76	45.0 ± 2.64
5	91.0 ± 2.6	45.0 ± 2.88
7	1.33 ± 0.80	1.4 ± 0.9

(Table 2). These outcomes could agree with very recently reported data[6] showing that the dimerization of two uSTAT3 monomers is energetically less favored compared with the binding of the pSTAT3 monomers. Thus, our weak ligands could negatively modulate uSTAT3. It is noteworthy that our simplified 1,4-dimethyl-carbazoles present a comparable inhibitory activity (> 90%) towards STAT3 respect to the previously reported compounds **11** and **12** (Figure S1 Supporting Information).[29]

4 Conclusions

We have shown that the simplified 1,4-dimethyl-carbazoles are suitable scaffold to develop STAT3 inhibitors. Our analysis suggests that the chlorine, methoxyl, ethyl ester are optimal substituents at C-6 to mimic to Tyr705/pTyr705. On the other hand, while our theoretical analysis also suggests the sulfonamide group as suitable for interacting with the macromolecular counterpart, a minor influence on the biological activity has been revealed by the experimental data. New studies are in progress to further evaluate the interactions of sulfonamide and other substituents with STAT3 also exploring different positions on the carbazole scaffold. Our outcomes show the relevant role, for the binding to the protein, of the hydrogen bond formed by NH and Ser636, suggesting the presence of a H-bond donor in position 9. Moreover, substituents at C-3 could be inserted to give other important interactions with Arg595, improving the binding affinity for STAT3. Even though **1**–**10** showed a modest potency, our aim was to simplify the carbazole core, in the context of our ongoing project to develop more potent and druggable inhibitors of STAT3. Moreover, the Western blot analysis highlights a relevant inhibition of STAT3 and not of pSTAT3, prompting us to further improve the biological activity of carbazole-based compounds. These results are in agreement with the reported evidence of a weaker protein-protein binding affinity between uSTAT3 monomers compared to phosphorylated ones. Thus, our weak binders could interfere with the unphosphorylated STAT3. Our data are the first example of unphosphorylated STAT3 modulation by small molecules, opening a new and complementary strategy to inhibit STAT3. It is noteworthy that the used chemical scaffold can be easily substituted in different positions, such as 1,3,4,8 allowing the chemical diversity exploration and increasing the possibility to obtain more promising STAT3 ligands. On the next generations of higher affinity ligands we will extend the evaluation of their STAT3 inhibitory activity in vivo.

Conflict of Interest

The authors declare no competing financial interest.

References

[1] J. E. Jr Darnell, *Science* **1997**, *277*, 1630 – 1635.
[2] J. N. Ihle, *Cell* **1996**, *84*, 331 – 334.
[3] S. Pellegrini, I. Dusanter-Fourt, *Eur. J. Biochem.* **1997**, *248*, 615 – 633.
[4] J. J. Darnell, I. Kerr, G. Stark, *Science* **1994**, *264*, 1415 – 1421.
[5] Z. Zhong, Z. Wen, J. Darnell, *Science* **1994**, *264*, 95 – 98.
[6] E. Nkansah, R. Shah, G. W. Collie, G. N. Parkinson, J. Palmer, K. M. Rahman, T. T. Bui, A. F. Drake, J. Husby, S. Neidle, G. Zinzalla, D. E. Thurston, A. F. Wilderspin, *FEBS Lett.* **2013**, *587*(7), 833 – 839.
[7] J. Yang, M. Chatterjee-Kishore, S. M. Staugaitis, H. Nguyen, K. Schlessinger, D. E. Levy, G. R. Stark, *Cancer Res.* **2005**, *65*, 939 – 947.
[8] J. Yang, X. Liao, M. K. Agarwal, L. Barnes, P. E. Auron, G. R. Stark, *Genes Dev.* **2007**, *21*, 1396 – 1408.
[9] J. B. Yang, G. R. Stark, *Cell Res.* **2008**, *18*, 443 – 451.
[10] H. Yu, R. Love, *Nat. Rev. Cancer* **2004**, *4(2)*, 97 – 105.
[11] R. Garcia, C. Yu, A. Hudnall, R. Catlett, K. Nelson, T. Smithgall, D. Fujita, S. Ethier, R. Jove, *Cell Growth Differ.* **1997**, *8*, 1267 – 1275.
[12] T. Bowman, R. Garcia, J. Turkson, R. Jove, *Oncogene* **2000**, *19*, 2474 – 2488.
[13] A. Lavecchia, C. Di Giovanni, E. Novellino, *Curr. Med. Chem.* **2011**, *18*, 2359 – 2375.
[14] P. K. Mandal, F. Gao, Z. Lu, Z. Ren, R. Ramesh, J. S. Birtwistle, K. K. Kaluarachchi, X. Chen, R. C. Bast, W. S. Liao, J. S. McMurray, *J. Med. Chem.* **2011**, *54*, 3549 – 3563.
[15] P. K. Mandal, Z. Ren, X. Chen, C. Xiong, J. S. McMurray, *J. Med. Chem.* **2009**, *52*, 6126 – 6141.
[16] A. Liu, Y. Liu, Z. Xu, W. Yu, H. Wang, C. Li, J. Lin, *Cancer Sci.* **2011**, *102*, 1381 – 1387.
[17] Y. Liu, A. Liu, Z. Xu, W. Yu, H. Wang, C. Li, J. Lin, *Apoptosis* **2011**, *16*, 502 – 510.
[18] H. Song, R. Wang, S. Wang, J. Lin, G. R. Stark, *Proc. Natl. Acad. Sci. USA* **2005**, *102*, 4700 – 4705.
[19] J. Schust, B. Sperl, A. Hollis, T. U. Mayer, T. Berg, *Chem. Biol.* **2006**, *13*, 1235 – 1242.
[20] L. Lin, B. Hutzen, P.-K. Li, S. Ball, M. Zuo, S. DeAngelis, E. Foust, M. Sobo, L. Friedman, D. Bhasin, L. Cen, C. Li, J. Lin, *Neoplasia* **2010**, *12*, 39 – 50.
[21] K. Siddiquee, S. Zhang, W. C. Guida, M. A. Blaskovich, B. Greedy, H. R. Lawrence, M. L. R. Yip, R. Jove, M. M. McLaughlin, N. J. Lawrence, S. M. Sebti, J. Turkson, *Proc. Natl. Acad. Sci. USA* **2007**, *104*, 7391 – 7396.
[22] W. Yu, H. Xiao, J. Lin, C. Li, *J. Med. Chem.* **2013**, *56*(11), 4402 – 4412.
[23] J. Turkson, S. Zhang, J. Palmer, H. Kay, J. Stanko, L. B. Mora, S. Sebti, H. Yu, R. Jove, *Mol. Cancer. Ther.* **2004**, *3(3)*, 1533 – 1542.
[24] J. Turkson, S. Zhang, L. B. Mora, A. Burns, S. Sebti, R. Jove, *J. Biol. Chem.* **2005**, *280*(38), 32979 – 32998.
[25] N. Jing, D. J. Tweardy, *Anticancer Drugs* **2005**, *16(6)*, 601 – 607.
[26] M. A. Blaskovich, J. Sun, A. Cantor, J. Turkson, R. Jove, M. S. Sebti, *Cancer Res.* **2003**, *63(15)*, 1270 – 1279.
[27] J. Sun, M. A. Blaskovich, R. Jove, S. K. Livingston, D. Coppola, S. M. Sebti, *Oncogene* **2005**, *24(20)*, 3236 – 3245.
[28] S. Nam, R. Buettner, J. Turkson, D. Kim, J. Q. Cheng, S. Muehlbeyer, F. Hippe, S. Vatter, K. H. Merz, G. Eisenbrand, R. Jove, *Proc. Natl. Acad. Sci. USA* **2005**, *102*(17), 5998 – 6003.
[29] C. Saturnino, C. Palladino, M. Napoli, M. S. Sinicropi, A. Botta, M. Sala, A. Carcereri de Prati, E. Novellino, H. Suzuki, *Eur. J. Med. Chem.* **2013**, *60*, 112 – 119.

[30] C. Saturnino, P. Longo, H. Suzuki, A. Carcereri de Prati, S. L. Nori, V. Nicolin, *Ital. Appl.* **2011**, IT SA20110014, IO 25820.
[31] J. L. Arbiser, B. Govindarajan, T. E. Battle, R. Lynch, D. A. Frank, M. Ushio-Fukai, B. N. Perry, D. F. Stern, G. T. Bowden, A. Liu, E. Klein, P. J. Kolodziejski, N. T. Eissa, C. F. Hossain, D. G. Nagle, *Invest. Dermatol.* **2006**, *126*, 1396 – 1402.
[32] R. Akué-Gédu, L. Nauton, V. Théry, J. Bain, P. Cohen, F. Anizon, P. Moreau, *Bioorg. Med. Chem.* **2010**, *18*, 6865 – 6873.
[33] H. A. Tran-Thi, T. Nguyen-Thi, S. Michel, F. Tillequin, M. Koch, B. Pfeiffer, A. Pierré, H. Trinh-Van-Dufat, *Chem. Pharm. Bull.* **2004**, **52**, 540 – 545.
[34] V. MoinetHedin, T. Tabka, P. Gauduchon, J. Y. Le Talaer, C. Saturnino, B. Letois, J. C. Lancelot, M. Robba, *Eur. J. Med. Chem.* **1997**, *32*, 113 – 122.
[35] L. Nagarapu, H. K. Gaikwad, K. Sarikonda, J. Mateti, R. Bantu, P. S. Raghu, K. M. Manda, S. V. Kalvendi, *Eur. J. Med. Chem.* **2010**, *45*, 4720 – 4725.
[36] *MacroModel*, Version 8.5, Schrödinger, LLC, New York, NY, **2003**.
[37] T. A. Halgren, *J. Comput. Chem.* **1996**, *17*, 616 – 641.
[38] W. C. Still, A. Tempczyk, R. C. Hawley, T. Hendrickson, *J. Am. Chem. Soc.* **1990**, *112*, 6127 – 6129.
[39] S. Becker, B. Groner, C. W. Muller, *Nature* **1998**, *394*, 145 – 151.
[40] G. M. Morris, R. Huey, W. Lindstrom, M. F. Sanner, R. K. Belew, D. S. Goodsell, A. J. Olson, *J. Comput. Chem.* **2009**, *16*, 2785 – 2791.
[41] P. A. Cranwell, J. E. Saxton, *J. Chem. Soc.* **1962**, 3482 – 3487

Received: April 16, 2015
Accepted: May 5, 2015
Published online: July 1, 2015

